Journal of Integrative Neuroscience

J. Integr. Neurosci. **2026**; 25(5): 48598
https://doi.org/10.31083/JIN48598

Original Research

Lactobacillus mucosae Reduces Neuronal Oxidative Stress in Alzheimer's Disease via the Regulation of CB2 Signaling

Yu Kong[1,†], Xinhuang Lv[2,†], Yao Yang[1], Qiyao Li[2], Conghui Dai[1], Xiaoou Lin[1], Jiaming Liu[1,*], Jing Li[3,*]

[1]Department of Preventive Medicine, School of Public Health, Wenzhou Medical University, 325027 Wenzhou, Zhejiang, China
[2]Department of Neurology, The Second Affiliated Hospital of Wenzhou Medical University, 325000 Wenzhou, Zhejiang, China
[3]Department of Neurology, The First Affiliated Hospital of Wenzhou Medical University, 325027 Wenzhou, Zhejiang, China
*Correspondence: wzjiaming_liu@163.com (Jiaming Liu); dami663@126.com (Jing Li)
[†]These authors contributed equally.
Academic Editor: Bettina Platt
Submitted: 27 November 2025 Revised: 9 February 2026 Accepted: 11 March 2026 Published: 19 May 2026

Abstract

Background: The probiotic *Lactobacillus mucosae* has been widely shown to have many positive effects. However, its neuroprotective effects and underlying mechanism in Alzheimer's disease (AD) remain elusive. **Methods**: Male APP/PS1 mice were treated for 4 weeks with *L. mucosae* WMU007, followed by the evaluation of cognitive function, neuronal damage, amyloid-β (Aβ) deposition, and Tau phosphorylation. RNA-seq coupled with Gene Ontology (GO) enrichment analysis implicated *L. mucosae* WMU007 in modulating oxidative stress in this AD model. Kyoto Encyclopedia of Genes and Genomes (KEGG) pathway analysis and qPCR were performed to identify the specific mechanism by which this probiotic suppresses oxidative stress in the pathogenesis of AD. In addition, we quantified the levels of classical oxidative stress markers, such as superoxide dismutase 2 (SOD2) and glutathione peroxidase 4 (GPX4). We also examined the expression of cannabinoid receptor type 2 (CB2) and its key downstream regulators in the redox pathway, namely nuclear factor erythroid 2-related factor 2 (Nrf2) and heme oxygenase 1 (HO-1), in both animal and cellular models. **Results**: Our results showed that treatment with *L. mucosae* WMU007 significantly decreased cognitive impairment, neuronal damage, Aβ deposits, and Tau phosphorylation in APP/PS1 mice. Activation of CB2 was identified as the key mechanism by which *L. mucosae* WMU007 reduces oxidative stress in AD. In addition, *L. mucosae* WMU007 reduced oxidative stress and increased the levels of CB2 pathway-related proteins *in vivo* and *in vitro*. **Conclusions**: These results indicate that *L. mucosae* WMU007 confers neuroprotection in AD by targeting CB2-mediated oxidative pathways, highlighting its therapeutic potential as a novel probiotic intervention.

Keywords: Alzheimer's disease; cannabinoid receptor type 2; *Lactobacillus mucosae*; neuroprotective effects; oxidative stress

1. Introduction

Alzheimer's disease (AD) is a progressive neurodegenerative disorder and the leading cause of dementia. AD is primarily characterized by cognitive impairment, and its incidence is rising with the aging of the global population [1–3]. The pathogenesis of AD is multifactorial and involves processes such as amyloid-β (Aβ) deposition, abnormal Tau phosphorylation, oxidative damage, and environmental risk factors [4]. Despite extensive research, effective therapeutic strategies for AD remain elusive. Oxidative stress resulting from excessive generation of reactive oxygen species (ROS) relative to the capacity of antioxidant systems is increasingly recognized as a key driver of the progression of AD [4,5]. Cellular redox balance is maintained by multiple antioxidant mechanisms, including enzymatic and non-enzymatic components that limit ROS accumulation, such as superoxide dismutase (SOD), glutathione peroxidase (GPX), and glutathione (GSH) [6]. Evidence from animal models and human studies has revealed elevated levels of lipid and protein oxidative damage in AD, supporting a role for oxidative injury in neurodegeneration [7,8]. An increasing number of studies suggest that alterations to gut microbiota are associated with the pathogenesis of AD [9,10]. The intestinal epithelium has also been reported to generate ROS in the presence of microbiota [11]. Certain probiotic strains, including *Bifidobacteria* and *Lactobacilli*, can modulate redox balance by regulating the production of nitric oxide (NO) [12]. As gut microbiota has been increasingly implicated in the regulation of oxidative stress, the identification of specific bacteria associated with these effects could open new avenues for therapeutic interventions.

Probiotics are live bacteria that interact with the intestinal environment and influence brain function through the bidirectional gut-brain communication axis [13]. *Lactobacillus mucosae* WMU007, a probiotic bacterium from the healthy human gut, has recently attracted increasing attention [14]. Oral administration of *Lactobacillus mucosae* NK41 alleviated cognitive deficits and Aβ accumulation in 5 $\times$ FAD-transgenic mice [15]. In a murine model of depression, *Lactobacillus* was reported to regulate the bioavailability of endocannabinoid precursors and to en-

hance hippocampal neurogenesis by increasing the level of endocannabinoids [16]. Cannabinoid receptor type 2 (CB2), a G-protein-coupled receptor [17], has been observed in association with senile plaque pathology in AD patients [18], suggesting a potential involvement in AD pathology. In the rotenone-induced Parkinson's disease model, activation of CB2 was shown to attenuate oxidative stress by preventing glutathione depletion, reducing lipid peroxidation, and enhancing antioxidant enzyme activity [19]. Treatment with *Lactobacillus acidophilus* increased the expression of CB2, ultimately reducing abdominal pain in rats [20]. Moreover, substantial evidence indicates that *Lactobacillus* enhances nuclear factor erythroid 2-related factor 2 (Nrf2) signaling and increases GPX4 levels [21], supporting its potential to mitigate oxidative stress. However, the mechanism by which *L. mucosae* activates CB2 and how this contributes to the attenuation of oxidative damage in AD remains poorly understood.

In this study, we examined the impact of *L. mucosae* WMU007 on cognitive impairment and pathological changes in the APP/PS1 mouse model. We elucidated the role of *L. mucosae* WMU007 in modulating oxidative stress in this AD model. The levels of oxidative stress-related proteins (SOD2 and GPX4) following treatment with *L. mucosae* WMU007 were also evaluated, allowing us to identify the potential mechanism by which *L. mucosae* attenuates oxidative stress. The expression of CB2 and downstream redox regulators, including Nrf2 and heme oxygenase 1 (HO-1), was also assessed. We demonstrated that *L. mucosae* WMU007 could inhibit oxidative stress via CB2-mediated signaling in APP/PS1 mice. This comprehensive study of how the specific microbiota *L. mucosae* influences oxidative stress and AD progression offers new insights into its therapeutic potential for AD.

2. Materials and Methods

2.1 Bacterial Culture

L. mucosae WMU007 was deposited in the China General Microbiological Culture Collection Centre (CGMCC). The strain was cultured in MRS broth (HB0384-1, HopeBio, Qingdao, China) under aerobic conditions at 37 °C for 24 h. Bacterial cells were collected by centrifugation (5000 rpm) and subsequently suspended in phosphate-buffered saline (PBS, ST477, Beyotime, Shanghai, China) to obtain a final density of 1×10^9 CFU/mL. *L. mucosae* WMU007 was cultured in MRS broth under aerobic conditions at 37 °C for 24 h, and the supernatant was filtered through a 0.22 µm membrane and diluted to 20% with sterile PBS, which was then used for the cell experiments.

2.2 Animals and Treatments

All experimental animals, including 6-month-old male APP/PS1 transgenic mice and C57BL/6J mice, were obtained from the Hangzhou Ziyuan Laboratory Animal Technology Co., Ltd. (Hangzhou, Zhejiang, China). The mice were housed under controlled environmental conditions, including an ambient temperature of 20–22 °C and a relative humidity maintained at approximately 50%. A 12-hour light/dark cycle was applied, with illumination from 08:00 to 20:00, and animals had ad libitum access to standard chow and drinking water. The mice were randomly divided into three groups: the WT group, the APP/PS1 group, and the *L. mucosae WMU007*-treated group (APP/PS1 + WMU007 group). Mice in the APP/PS1 + WMU007 group were intragastrically administered *L. mucosae* WMU007 for 4 weeks, while mice in the WT and APP/PS1 groups received an equal volume of PBS as a control. All mice were gavaged with 8 mg arachidonic acid (A131025, Aladdin, Shanghai, China) before *L. mucosae* WMU007 or PBS treatment. Then, all mice underwent behavioral evaluation, such as the Nesting behavior test, novel object recognition test (NORT), and open field test (OFT).

2.3 Novel Object Recognition Test (NORT)

The NORT was applied to assess the memory and cognitive abilities of mice. Two identical cuboids were symmetrically placed (5 cm from the edges of the field) in an open field with a bottom side length of 25 cm, a height of 25 cm, and each mouse was permitted to explore the open field without restriction for 5 min. The next day, one of the cuboids was replaced with a cylinder of the same material with a bottom diameter of 3 cm, a height of 6 cm, and each mouse was allowed to explore freely for 5 min. After the mouse completed the test, the equipment was wiped with 75% alcohol to eliminate odor interference. Then, the time of the mouse exploring the cylinder (defined as TN) and the cuboid (defined as TF) were calculated. Mice sniffing and lying on objects were defined as exploration; the discriminant index (DI) = (TN – TF) / (TN + TF) × 100% was used for data analysis.

2.4 Nesting Behavior Test

Nesting behavior, which is closely associated with hippocampal function in rodents, was assessed using a nesting test. Thirty squares of paper (each measuring 5 cm × 5 cm) were distributed throughout the home cage of each mouse. Animals were allowed to move freely within the cage, and nest construction was documented after 24 h. The nesting performance was scored based on the scoring criteria as follows: (1) no visible nest; (2) no obvious nest, paper occupying more than 1/3 of the cage bottom; (3) obvious nest, paper accounting for 1/4 – 1/3 of the cage bottom; (4) obvious nest, paper occupying less than 1/4 of the cage bottom.

2.5 Open Field Test (OFT)

The OFT was carried out to measure the exploratory behavior and curiosity of mice towards the new environment. Each mouse was placed in an open field with a side

length of 20 cm at the bottom and a height of 30 cm, and permitted to explore freely for 5 min. The active time and rest time of mice were quantified using the Digbehv Animal Behavior Analysis System (version 2.0, Shanghai Jiliang Software Technology Co., Ltd., Shanghai, China). At the end of each test, the open-field apparatus was cleaned with 75% ethanol and allowed to air-dry to prevent potential olfactory cues from influencing subsequent tests.

2.6 Western Blot

After behavioral testing, mice were deeply anesthetized by intraperitoneal injection of pentobarbital sodium (P3761, Sigma-Aldrich, St. Louis, MO, USA) (50 mg/kg). Adequate anesthesia was confirmed by the absence of the pedal withdrawal reflex. The mice were then euthanized by cervical dislocation, and brain tissues were quickly collected. The brain tissue was quickly removed and thoroughly homogenized in a RIPA Lysis Buffer (P0013B, Beyotime, Shanghai, China) mixed with PMSF and Protein Phosphatase Inhibitor (P1260, Solarbio, Beijing, China), centrifuged at 4 °C at 12,000 rpm for 30 min, and the supernatant was removed. The total protein concentration was measured by the Enhanced BCA Protein Assay Kit (P0010, Beyotime, Shanghai, China), and the sample was denatured at 95 °C for 5 min with the SDS-PAGE Sample Loading Buffer (P0015L, Beyotime, Shanghai, China). The 40 µg of protein from each sample were added to 10% SDS-PAGE gel system for electrophoretic separation and transferred to the PVDF membrane. Then, the membrane was sealed in 5% skim milk at room temperature for 1 h, and incubated with the following primary antibodies at 4 °C overnight: Aβ_{1-42} (1:1000, #14974, Cell Signaling Technology, Danvers, MA, USA), phospho-Tau231 (1:1000, BS4252, Bioworld, Bloomington, MN, USA), Tau (1:1000, BS1358, Bioworld), SOD2 (1:1000, BS6734, Bioworld), CB2 (1:1000, BS72034, Bioworld), Nrf2 (1:1000, BS1258, Bioworld), GPX4 (1:1000, BS7323, Bioworld), HO-1 (1:1000, BS6626, Bioworld), Gapdh (1:5000, AP0063, Bioworld), β-actin (1:1000, AP0060, Bioworld). Then, the membrane was uniformly covered with Super-sensitive ECL chemiluminescent substrate (BL520B, Biosharp, Hefei, Anhui, China). The grayscale value analysis was performed with ImageJ software (version 1.54, National Institutes of Health, Bethesda, MD, USA). The original images were in the **Supplementary Materials**.

2.7 Immunofluorescence

The brain tissue of mice was fixed in 4% PFA (P0099, Beyotime), dehydrated by gradient alcohol, cleared in xylene (Changshu Hongsheng Fine Chemical Co., Ltd., Changshu, Jiangsu, China), and embedded after wax immersion. The wax block was cut into pieces of 5 µm, heated at 65 °C for 2 h, dewaxed in xylene for 30 min, and rehydrated through a graded ethanol series. Then, the sections were repaired with the antigen via the Hotfix method, soaked in sodium citrate buffer, heated in a pressure cooker for 5 min, left for 10 min, and applied for subsequent staining until cooled to room temperature. Next, the sections were permeabilized with 0.3% Triton for 15 min, blocked in 10% BSA for 1 h, and incubated overnight at 4 °C with primary antibodies, including NeuN (1:200, HA601111, HUABIO, Hangzhou, China), Aβ_{1-42} (1:400, #14974, Cell Signaling Technology) and SOD2 (1:200, BS6734, Bioworld). Subsequently, the pieces were equilibrated at 37 °C for 30 min, followed by incubation with the corresponding secondary antibody for 1 h under light-protected conditions. The samples were then rinsed with PBS for 3 $\times$ 5 min. Nuclear counterstaining was performed using DAPI staining solution (C1006, Beyotime) for 5 min. After extensive PBS washes, the sections were mounted using an antifade mounting medium (P0126, Beyotime). Fluorescent signals of the target proteins were visualized using a fluorescence microscope (DM4000 B LED, Leica Microsystems CMS GmbH, Wetzlar, Germany).

2.8 Cells Culture and Treatment

N2a cells were obtained from the National Collection of Authenticated Cell Cultures (Shanghai, China), which provides STR-authenticated cell lines. All cell lines were routinely tested for mycoplasma contamination using a PCR-based detection kit, and all results were negative. APP/SWE cells were generated by transient transfection of N2a cells at 60% confluency with 0.5 µg APPswe695 plasmid using PEI Transfection Reagent (HY-W250110, MCE, Princeton, NJ, USA) and were pretreated with DMEM (C0891, Beyotime) medium containing 20% *L. mucosae* WMU007 fermentation for 8 h.

2.9 ROS Detection

The N2a cells were cultured in serum-free medium and exposed to the DCFH-DA probe (S1105S, Beyotime) at 37 °C for 20 min. Subsequently, nuclear counterstaining was carried out using Hoechst dye (C1011, Beyotime), and intracellular fluorescence signals were captured and quantified under a fluorescence microscope.

2.10 RNA Sequencing and Data Analysis

Total RNA was isolated from mouse cerebral cortex samples with TRIzol reagent (Invitrogen, Thermo Fisher Scientific, Waltham, MA, USA) following standard protocols. The RNA's concentration, purity, and integrity were then assessed. Procedures including mRNA enrichment, RNA fragmentation, reverse transcription, library construction, and high-throughput sequencing were completed by Shanghai Majorbio Bio-pharm Biotechnology Co., Ltd. (Shanghai, China). To ensure the reliability of downstream bioinformatics analyses, raw sequencing reads were subjected to quality control using fastp (OpenGene, GitHub, San Francisco, CA, USA). Clean reads with high quality

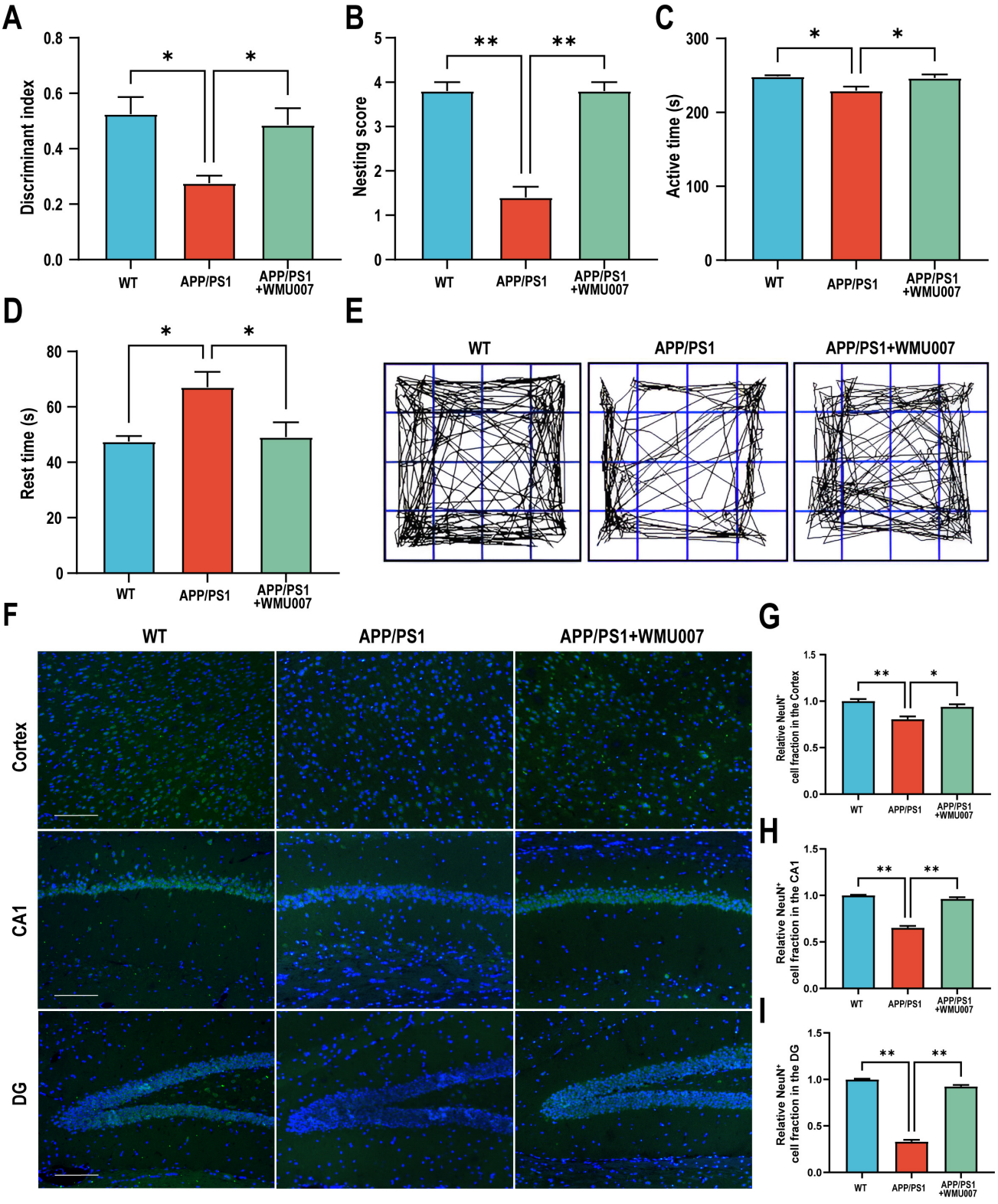

Fig. 1. *L. mucosae* WMU007 treatment improved cognitive dysfunction in APP/PS1 mice (n = 5 mice per group). (A) The discriminant index in NORT. (B) The nesting score in the Nesting Behavior Test. (C) The active time in the open field test. (D) The rest time in the open field test. (E) Representative images of activity trajectory in the open field test. (F) Representative images of NeuN staining (green) in the cortex and hippocampus (CA1, DG), counterstained with DAPI (blue). Magnification, 200×. Scale bars, 100 μm. (G–I) Quantification of relative $NeuN^+$ cell fraction in the cortex (G), CA1 (H), and DG (I) (n = 3). Data are shown as mean ± SEM. *p*-values were determined by one-way ANOVA. *: $p < 0.05$, **: $p < 0.01$.

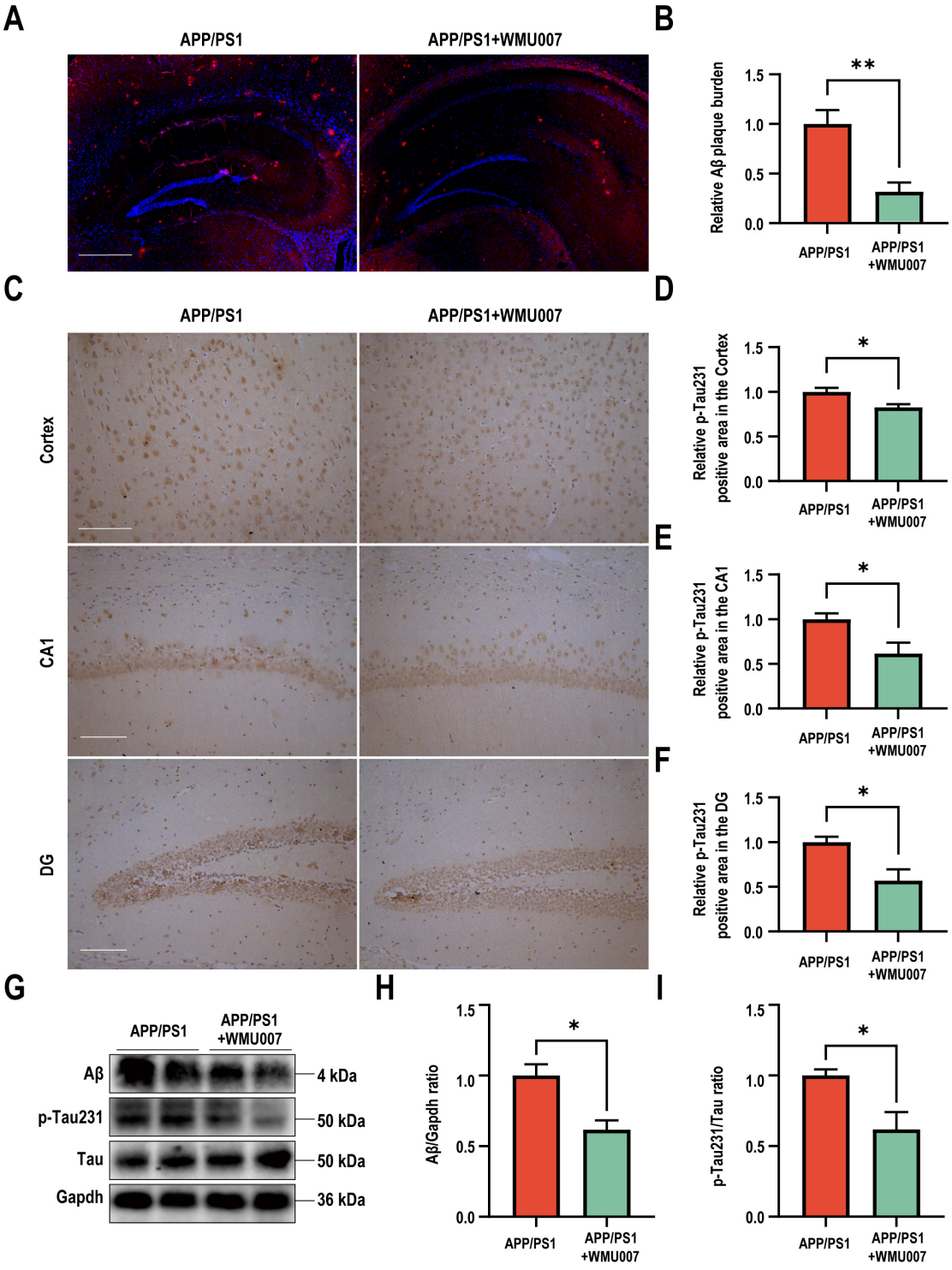

Fig. 2. *L. mucosae* WMU007 treatment improved neuronal damage and decreased Aβ deposition and Tau hyperphosphorylation in APP/PS1 mice. (A) Representative immunofluorescence images of Aβ (red) in hippocampal regions from the APP/PS1 group and APP/PS1 + WMU007 group, counterstained with DAPI (blue). Magnification, 50×. Scale bars, 400 µm. (B) Quantification of relative Aβ plaque (n = 3). (C) Representative immunohistochemical images of Tau in the cortex and hippocampus (CA1, DG), counterstained with DAPI (blue). Magnification, 200×. Scale bars, 100 µm. (D–F) Quantification of relative p-Tau231-positive area in the cortex (D), CA1 (E), and DG (F) (n = 3). (G) Representative western blot images of Aβ, p-Tau231, and Tau. (H,I) Quantitative analysis of Aβ, p-Tau231, and Tau expression (n = 4). The ratio of Aβ/Gapdh and p-Tau231/Tau in the APP/PS1 group were used as the reference value. Data are shown as mean ± SEM. *p*-values were determined by the *t*-test. $^{*}p < 0.05$ vs. APP/PS1 group, $^{**}p < 0.01$ vs. APP/PS1 group.

were then *de novo* assembled using the Trinity platform. The preliminary assembled sequences underwent refinement and filtering via TransRate (http://hibberdlab.com/transrate/). The completeness of the assembled transcripts was further evaluated with BUSCO (Benchmarking Universal Single-Copy Orthologs). Differential gene expression analysis was performed using the DESeq2 package (Bioconductor, Seattle, Washington, USA), and genes meeting the criteria of $|\text{FoldChange}| > 0.3$ and $p\text{-value} < 0.05$ were defined as differentially expressed. Subsequently, GO and KEGG enrichment analyses were performed using the clusterProfiler package (version 4.16.0, Bioconductor), while gene set enrichment analysis (GSEA) was performed using the fgsea package (version 1.34.0, Bioconductor). Visualization of the results was accomplished using ggplot2 (version 3.5.2, CRAN, Vienna, Austria), pheatmap (version 1.0.13, CRAN), and other relevant packages mentioned above.

2.11 Real-time PCR

Real-time quantitative PCR was performed using ChamQ Universal SYBR qPCR Master Mix (Q711, Vazyme Biotech Co., Ltd., Nanjing, Jiangsu, China) according to the manufacturer's instructions. Relative gene expression was normalized to Actin and calculated using the $2^{-\Delta\Delta CT}$ method. The primer sequences were as follows: CB2-F, 5′-ACGGTGGCTTGGAGTTCAAC-3′; CB2-R, 5′-GCCGGGAGGACAGGATAAT-3′.

2.12 Statistical Analysis

Data were represented as mean ± SEM. All statistical evaluations were conducted using SPSS software (version 22.0, IBM SPSS Statistics, Chicago, IL, USA). Group differences were assessed by the *t*-test or one-way ANOVA. Statistical significance was defined as $p < 0.05$.

3. Results

3.1 L. mucosae WMU007 Treatment Improved Cognitive Dysfunction in APP/PS1 Mice

To investigate the effects of *L. mucosae* WMU007 treatment on cognitive dysfunction in APP/PS1 mice, a series of behavioral assessments was conducted. In NORT, the discrimination index of APP/PS1 mice was significantly lower than that of WT mice, while WMU007 treatment significantly increased the discrimination index compared with the APP/PS1 group ($p < 0.05$, Fig. 1A). In the Nesting behavior test, the nesting score of the WMU007-treated group was significantly higher than that of the APP/PS1 group ($p < 0.01$, Fig. 1B). In OFT, the active time of the WMU007 group was markedly longer than the APP/PS1 group ($p < 0.05$, Fig. 1C). In contrast, the rest time in the WMU007 group was significantly shorter than the APP/PS1 group ($p < 0.05$, Fig. 1D). The representative images of the activity trajectory of three groups are displayed in Fig. 1E. These findings suggested that *L. mucosae* WMU007 treatment significantly improved cognitive impairment.

3.2 L. mucosae WMU007 Treatment Improved Neuronal Damage and Decreased Aβ Deposition and Tau Hyperphosphorylation in APP/PS1 Mice

To assess the effects of *L. mucosae* WMU007 on neuropathological changes, NeuN staining, Aβ deposit, and tau phosphorylation were detected. The number of NeuN-positive neurons in the cortex, CA1, and DG of the *L. mucosae* WMU007-treated group was increased compared with the APP/PS1 group (Fig. 1F–I). Immunofluorescence analysis showed that Aβ plaque was markedly decreased in the *L. mucosae* WMU007-treated group compared with APP/PS1 mice (Fig. 2A,B). In addition, the level of Tau phosphorylation in *L. mucosae* WMU007-treated APP/PS1 mice was significantly decreased compared with APP/PS1 mice (Fig. 2C–F). In the Western blot, the level of Aβ in WMU007-treated group was significantly decreased compared with the APP/PS1 group ($p < 0.05$, Fig. 2G,H). The ratio of p-Tau231/Tau in the WMU007-treated group was remarkably reduced compared with that in APP/PS1 mice ($p < 0.05$, Fig. 2G–I). These findings suggested that *L. mucosae* WMU007 treatment improved neuropathological changes of AD.

3.3 L. mucosae WMU007 Fermentation Treatment Decreased Oxidative Stress In Vitro

To elucidate the molecular mechanism of *L. mucosae* WMU007 underlying the decreased Aβ deposition and Tau hyperphosphorylation, transcriptomic profiling was conducted to characterize gene expression changes between WMU007-treated and untreated groups. The analysis yielded a total of 231 upregulated genes and 365 downregulated genes ($|\log2FC| > 0.3$, $p < 0.05$). Differentially expressed genes between the two groups were visualized using a volcano plot (Fig. 3A), while hierarchical clustering of the top 30 DEGs was illustrated by a heatmap (Fig. 3B). To explore the functional implications of the *L. mucosae* WMU007 intervention, the GO enrichment analysis was conducted based on the identified DEGs. Biological Process annotation revealed that WMU007 predominantly modulated pathways related to oxidative stress (Fig. 3C). To further confirm the effect of *L. mucosae* WMU007 on oxidative stress, we performed an analysis of ROS, SOD2, and GPX4. The fluorescence staining showed that the level of ROS was decreased in the *L. mucosae*-treated group compared with the Con group in N2a cells ($p < 0.01$, Fig. 3D,E). Western blot analysis showed that the SOD2 and GPX4 levels were significantly increased in *L. mucosae*-treated N2a cells ($p < 0.01$, Fig. 3F–H). These findings suggested that *L. mucosae* WMU007 effectively decreased oxidative stress.

3.4 L. mucosae WMU007 Inhibited Oxidative Stress via Activating the CB2 Pathway

To further investigate the mechanism of *L. mucosae* WMU007 on inhibiting oxidative stress, KEGG enrichment analysis was conducted based on genes exhibiting al-

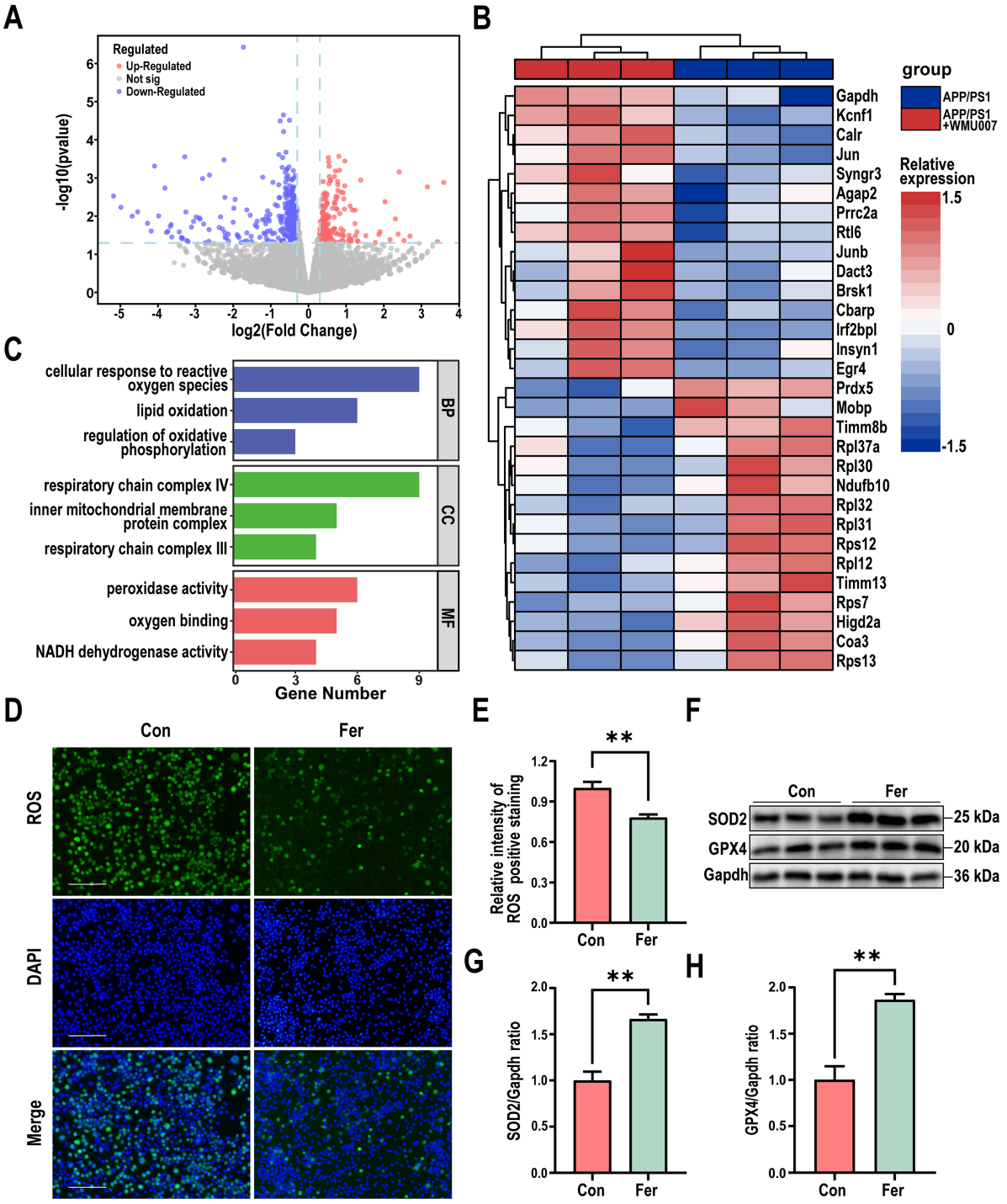

Fig. 3. *L. mucosae* WMU007 treatment decreased oxidative stress. (A) Volcano plot showing the distribution of gene expression level differences. p-value < 0.05 was screened as differentially expressed genes. (B) Heatmap showing differentially expressed genes. (C) GO analysis showing the biological functions of DEGs. Significant changes in oxidative stress-related pathways were found. (D) Representative images of ROS staining (green) of N2a cells in the Con group and the Fer group, counterstained with Hoechst (blue). Magnification, 100×. Scale bars, 200 μm. Fer, *L. mucosae* WMU007 fermentation. (E) Quantification of the relative intensity of ROS-positive staining (n = 6). (F) Representative western blot images of SOD2 and GPX4. (G,H) Quantitative analysis of SOD2 and GPX4 expression (n = 3). The ratio of SOD2/Gapdh and GPX4/Gapdh in Con group was used as the reference value. Data are shown as mean ± SEM. p-values were determined by the t-test. $^{**}p < 0.01$ vs. Con group. ROS, reactive oxygen species; SOD2, superoxide dismutase 2; GPX4, glutathione peroxidase 4; BP, biological process; CC, cellular component; MF, molecular function.

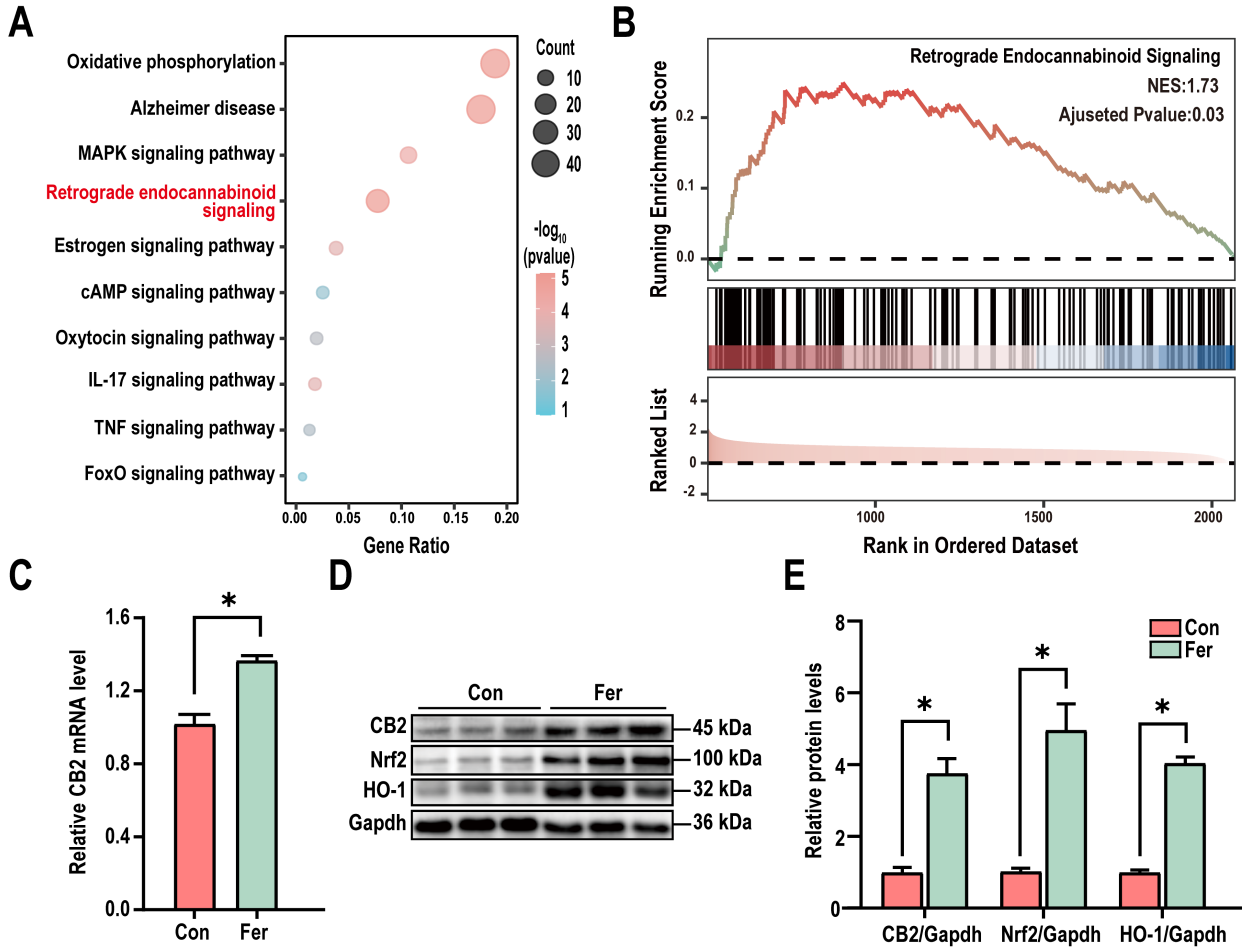

Fig. 4. *L. mucosae* WMU007 inhibited oxidative stress via activating the CB2 pathway. (A) KEGG pathway enrichment showing the Retrograde endocannabinoid signaling was significantly enriched in DEGs. p-value < 0.05 was considered statistically significant. (B) GSEA plot for the "Retrograde Endocannabinoid Signaling". (C) The relative expression levels of *CB2* mRNA between the Con group and the Fer group (n = 3), Fer, *L. mucosae* WMU007 fermentation. (D) Representative western blot images of CB2, Nrf2, and HO-1. (E) Quantitative analysis of CB2, Nrf2, and HO-1 expression (n = 3). The ratio of CB2/Gapdh, Nrf2/Gapdh, and HO-1/Gapdh in the Con group was used as the reference value. Data are shown as mean ± SEM. p-values were determined by the t-test. $^{*}p < 0.05$ vs. Con group. CB2, cannabinoid receptor type 2; Nrf2, nuclear factor erythroid 2-related factor 2; HO-1, heme oxygenase-1.

tered expression in the RNA-Seq results. KEGG analysis revealed significant differences in the Retrograde endocannabinoid signaling among the DEGs (Fig. 4A). To gain a more comprehensive understanding of the changes in the Retrograde endocannabinoid signaling, we conducted GSEA enrichment analysis. A normalized enrichment score (NES) of 1.73 indicates that *L. mucosae* treatment can significantly activate the aforementioned pathway (Fig. 4B). As shown in Fig. 4C, the qPCR analysis revealed a significant elevation of *CB2* transcript abundance in mice receiving *L. mucosae* WMU007 relative to controls ($p < 0.05$). To further investigate the effect of *L. mucosae* WMU007 on the CB2 signaling pathway, we examined the expression levels of key proteins associated with this pathway, including CB2, Nrf2, and HO-1. The Western blot analysis showed that the levels of CB2, Nrf2, and HO-1 were markedly increased after *L. mucosae* WMU007 treatment compared with the Con group ($p < 0.05$, Fig. 4D,E). Collectively, these findings indicate that *L. mucosae* supplementation attenuates oxidative stress by activating the CB2 signaling pathway *in vivo*.

3.5 L. mucosae WMU007 Treatment Reduces Oxidative Stress in APP/PS1 Mice via Activating the CB2 Pathway

To confirm the role of *L. mucosae* WMU007 in inhibiting oxidative stress through CB2 receptor activation, APP/PS1 mice were treated with *L. mucosae* WMU007. Immunofluorescence staining revealed a significant increase in SOD2-positive fluorescence intensity in the cortex, CA1, and DG of the *L. mucosae* WMU007-treated group compared to the APP/PS1 group (Fig. 5A–D). To further assess antioxidant responses and CB2 signaling, we analyzed protein expression by Western blot. Our results showed that *L. mucosae* WMU007 treatment significantly

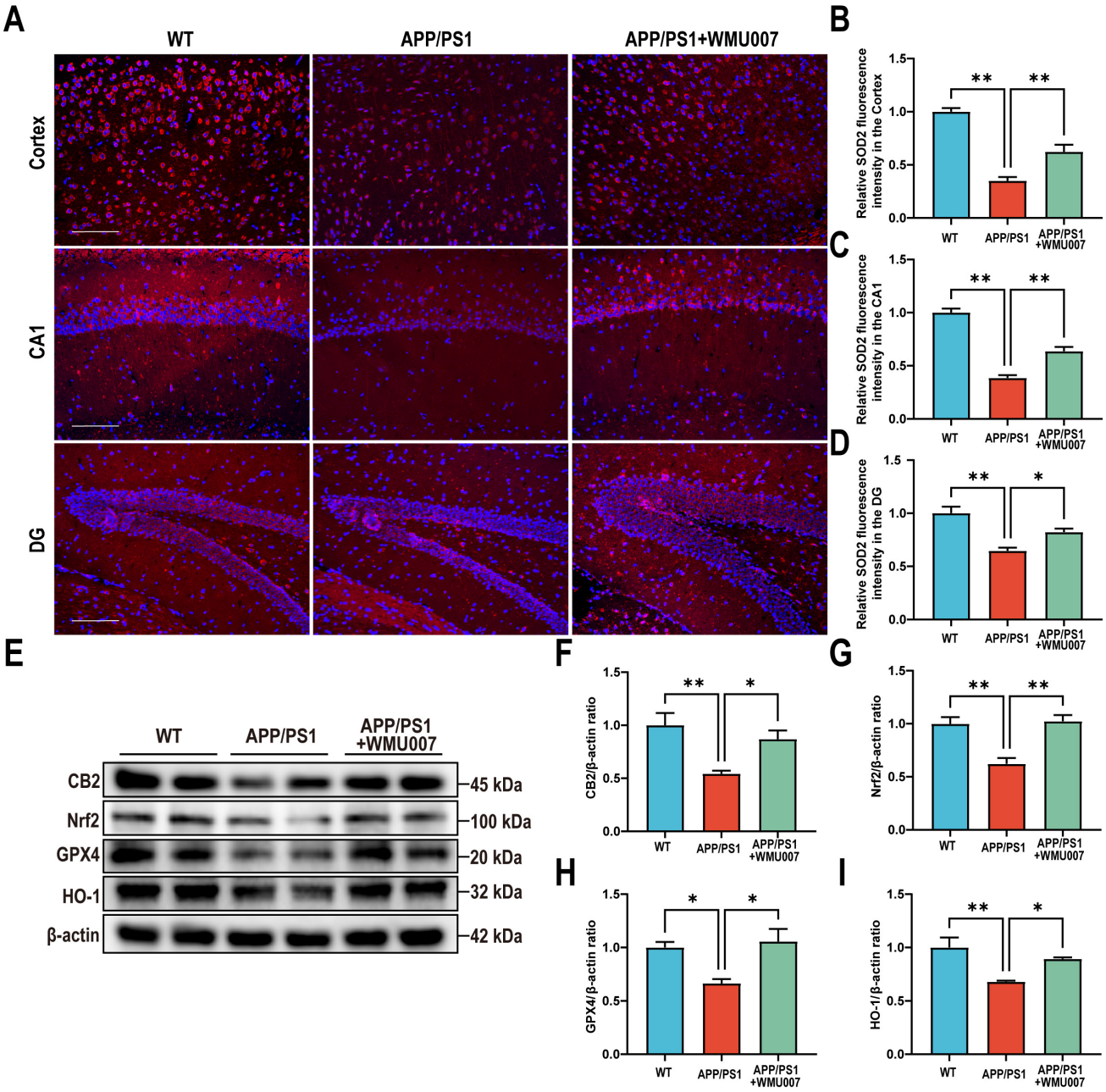

Fig. 5. ***L. mucosae*** **WMU007 treatment reduces oxidative stress in APP/PS1 mice via activating the CB2 pathway.** (A) Representative immunofluorescence images of SOD2 (red) in the cortex and hippocampal (CA1 and DG) regions, counterstained with DAPI (blue). Magnification, 200×. Scale bars, 100 µm. (B–D) Quantification of relative SOD2 fluorescence intensity in the cortex (B), CA1 (C), and DG (D) (n = 3). (E) Representative western blot images of CB2, Nrf2, GPX4, and HO-1. (F–I) Quantitative analysis of CB2, Nrf2, GPX4 and HO-1 expression (n = 4). The ratio of CB2/β-actin, Nrf2/β-actin, GPX4/β-actin, and HO-1/β-actin in the WT group was used as the reference value. Data are shown as mean ± SEM. p-values were determined by one-way ANOVA. *: $p < 0.05$, **: $p < 0.01$.

increased the levels of CB2, Nrf2, GPX4 and HO-1 compared to the APP/PS1 group (CB2: $p < 0.05$, Nrf2: $p < 0.01$, GPX4: $p < 0.05$, HO-1: $p < 0.05$, Fig. 5E–I). These findings suggested that the potential mechanism by which *L. mucosae* WMU007 alleviated oxidative stress might be related to regulating CB2 signaling.

4. Discussion

This study revealed that *L. mucosae* WMU007 confers protective effects against oxidative stress in AD. Treatment with *L. mucosae* WMU007 significantly alleviated cognitive impairment, neuronal damage, and AD-related pathological changes in APP/PS1 mice. We found that

L. mucosae WMU007 was involved in regulating oxidative stress, a key factor in the progression of AD. Furthermore, activation of the CB2 receptor was identified as the key mechanism by which *L. mucosae* WMU007 inhibits oxidative stress in AD. Supplementation with *L. mucosae* WMU007 was confirmed to inhibit oxidative stress and increase CB2-associated protein levels, both *in vivo* and *in vitro*. The above findings suggest that *L. mucosae* WMU007 may inhibit oxidative stress in AD through the CB2-mediated pathway.

Our study found that *L. mucosae* WMU007 could ameliorate cognitive impairment, reduce neuronal damage, and decrease Aβ deposition and Tau phosphorylation in a mouse model of AD. These results align with previous reports showing that oral administration of *Lactobacillus mucosae* NK41 alleviated cognitive dysfunction and reduced Aβ accumulation in 5×FAD transgenic mice [15]. Collectively, the findings suggest that *L. mucosae* exerts beneficial effects in AD by improving cognitive dysfunction and mitigating pathological changes. Oxidative stress, characterized by excessive ROS production and impaired antioxidant defenses, plays a pivotal role in the pathogenesis of AD [22]. Previous studies have reported decreased GPX4 levels accompanied by elevated ROS production and increased lipid peroxidation in AD patients [23–25]. More recently, *L. mucosae* was shown to exhibit antioxidant effects [14], which significantly increased serum glutathione peroxidase (GSH-Px) and reduced the MDA level in D-galactose-induced aging mice [26]. These findings indicated that *L. mucosae* WMU007 could inhibit oxidative stress of AD, but the mechanism still needs to be further clarified.

We identified CB2 activation as a key mechanism for inhibiting oxidative stress in AD. As members of the G-protein coupled receptor family, cannabinoid receptors were shown to participate extensively in central nervous system diseases [27]. Importantly, the expression level of CB2 has been associated with the Aβ_{42} level and elderly plaque score [28]. Previous studies demonstrated that MDA7 facilitates amyloid plaque clearance, restores synaptic plasticity, and improves behavioral outcomes in animal models [29,30]. Moreover, accumulating evidence indicates that CB2 activation participates in the regulation of oxidative stress [31,32]. Activated CB2 has been shown to reduce the formation of ROS/RNS, as well as lipid peroxidation [33]. The CB2 activator JWH-133 was found to reduce the level of 4-HNE and increase the expression of SOD1 and SOD2 in APP/PS1 mice [34]. The CB2 agonist AM1241 markedly increased Nrf2 activation and facilitated its translocation into the nucleus, leading to reduced ROS production [35]. *L. acidophilus* was also reported to stimulate the expression of *CB2* mRNA in resting HT-29 epithelial cells [20]. In the present study, we demonstrated that *L. mucosae* WMU007 could increase the level of CB2 and reduce downstream redox regulators, both *in vivo* and *in vitro*. These findings confirm that CB2 activation is a potent antioxidant pathway in AD, and identify *L. mucosae* as a promising microbial modulator of this neuroprotective mechanism.

5. Limitation

Although the results supported protective effects of *L. mucosae* WMU007 in the AD models and suggested that CB2 activation might be a key mechanism, several limitations still need to be addressed. This study only used male mice; future research should include female animals to assess potential differences. Further long-term observations should be evaluated potential adverse effects.

6. Conclusions

In conclusion, this study revealed that *L. mucosae* WMU007 might be involved in the inhibition of oxidative stress by activating the CB2, ultimately improving the pathogenesis of AD. Our study provided insights into the association between *L. mucosae* and oxidative stress in AD, suggesting that specific probiotics may become a promising therapeutic target for AD.

Availability of Data and Materials

The datasets used during the current study are available from the corresponding author on reasonable request.

Author Contributions

JLiu and JLi conceived and designed the experiments. YK, XLv, YY, QL, CD and XLin performed the experiments and conducted the statistical analyses. All authors contributed to editorial changes in the manuscript. All authors have read and agreed to the published version of the manuscript. All authors have participated sufficiently in the work and agreed to be accountable for all aspects of the work.

Ethics Approval and Consent to Participate

All experiments were conducted in accordance with the National Institutes of Health Guide for the Care and Use of Laboratory Animals and under the guidance of the Animal Experiment Ethics Committee of First Affiliated Hospital of Wenzhou Medical University (No. WYYY-AEC-YS-2024-0378).

Acknowledgment

Not applicable.

Funding

This work was supported by Science and Technology Funds of Wenzhou (Y20240038).

Conflicts of Interest

The authors declare no conflicts of interest.

Supplementary Material

Supplementary material associated with this article can be found, in the online version, at https://doi.org/10.31083/JIN48598.

References

[1] Boxer AL, Sperling R. Accelerating Alzheimer's therapeutic development: The past and future of clinical trials. Cell. 2023; 186: 4757–4772. https://doi.org/10.1016/j.cell.2023.09.023.

[2] Lu S, Qiu S, Guan Y, Zhang A, Zhao Q. Tau phosphorylation homeostasis: Mechanisms, targets, and therapeutic implications in Alzheimer's disease. Ageing Research Reviews. 2026; 118: 103097. https://doi.org/10.1016/j.arr.2026.103097.

[3] Ward RJ, Zucca FA, Duyn JH, Crichton RR, Zecca L. The role of iron in brain ageing and neurodegenerative disorders. The Lancet. Neurology. 2014; 13: 1045–1060. https://doi.org/10.1016/S1474-4422(14)70117-6.

[4] Bai R, Guo J, Ye XY, Xie Y, Xie T. Oxidative stress: The core pathogenesis and mechanism of Alzheimer's disease. Ageing Research Reviews. 2022; 77: 101619. https://doi.org/10.1016/j.arr.2022.101619.

[5] Haque MM, Murale DP, Kim YK, Lee JS. Crosstalk between Oxidative Stress and Tauopathy. International Journal of Molecular Sciences. 2019; 20: 1959. https://doi.org/10.3390/ijms20081959.

[6] Jomova K, Alomar SY, Alwasel SH, Nepovimova E, Kuca K, Valko M. Several lines of antioxidant defense against oxidative stress: antioxidant enzymes, nanomaterials with multiple enzyme-mimicking activities, and low-molecular-weight antioxidants. Archives of Toxicology. 2024; 98: 1323–1367. https://doi.org/10.1007/s00204-024-03696-4.

[7] Loffredo L, Ettorre E, Zicari AM, Inghilleri M, Nocella C, Perri L, *et al*. Oxidative Stress and Gut-Derived Lipopolysaccharides in Neurodegenerative Disease: Role of NOX2. Oxidative Medicine and Cellular Longevity. 2020; 2020: 8630275. https://doi.org/10.1155/2020/8630275.

[8] Botchway BO, Okoye FC, Chen Y, Arthur WE, Fang M. Alzheimer Disease: Recent Updates on Apolipoprotein E and Gut Microbiome Mediation of Oxidative Stress, and Prospective Interventional Agents. Aging and Disease. 2022; 13: 87–102. https://doi.org/10.14336/AD.2021.0616.

[9] Vogt NM, Romano KA, Darst BF, Engelman CD, Johnson SC, Carlsson CM, *et al*. The gut microbiota-derived metabolite trimethylamine N-oxide is elevated in Alzheimer's disease. Alzheimer's Research & Therapy. 2018; 10: 124. https://doi.org/10.1186/s13195-018-0451-2.

[10] Sochocka M, Donskow-Łysoniewska K, Diniz BS, Kurpas D, Brzozowska E, Leszek J. The Gut Microbiome Alterations and Inflammation-Driven Pathogenesis of Alzheimer's Disease-a Critical Review. Molecular Neurobiology. 2019; 56: 1841–1851. https://doi.org/10.1007/s12035-018-1188-4.

[11] Shabbir U, Tyagi A, Elahi F, Aloo SO, Oh DH. The Potential Role of Polyphenols in Oxidative Stress and Inflammation Induced by Gut Microbiota in Alzheimer's Disease. Antioxidants (Basel, Switzerland). 2021; 10: 1370. https://doi.org/10.3390/antiox10091370.

[12] Oleskin AV, Shenderov BA. Neuromodulatory effects and targets of the SCFAs and gasotransmitters produced by the human symbiotic microbiota. Microbial Ecology in Health and Disease. 2016; 27: 30971. https://doi.org/10.3402/mehd.v27.30971.

[13] Loh JS, Mak WQ, Tan LKS, Ng CX, Chan HH, Yeow SH, *et al*. Microbiota-gut-brain axis and its therapeutic applications in neurodegenerative diseases. Signal Transduction and Targeted Therapy. 2024; 9: 37. https://doi.org/10.1038/s41392-024-01743-1.

[14] Kim JK, Lee KE, Lee SA, Jang HM, Kim DH. Interplay Between Human Gut Bacteria *Escherichia coli* and *Lactobacillus mucosae* in the Occurrence of Neuropsychiatric Disorders in Mice. Frontiers in Immunology. 2020; 11: 273. https://doi.org/10.3389/fimmu.2020.00273.

[15] Ma X, Kim JK, Shin YJ, Son YH, Lee DY, Park HS, *et al*. Alleviation of Cognitive Impairment-like Behaviors, Neuroinflammation, Colitis, and Gut Dysbiosis in 5xFAD Transgenic and Aged Mice by *Lactobacillus mucosae* and *Bifidobacterium longum*. Nutrients. 2023; 15: 3381. https://doi.org/10.3390/nu15153381.

[16] Chevalier G, Siopi E, Guenin-Macé L, Pascal M, Laval T, Rifflet A, *et al*. Effect of gut microbiota on depressive-like behaviors in mice is mediated by the endocannabinoid system. Nature Communications. 2020; 11: 6363. https://doi.org/10.1038/s41467-020-19931-2.

[17] Li Y, Kim J. Neuronal expression of CB2 cannabinoid receptor mRNAs in the mouse hippocampus. Neuroscience. 2015; 311: 253–267. https://doi.org/10.1016/j.neuroscience.2015.10.041.

[18] Ramírez BG, Blázquez C, Gómez del Pulgar T, Guzmán M, de Ceballos ML. Prevention of Alzheimer's disease pathology by cannabinoids: neuroprotection mediated by blockade of microglial activation. The Journal of Neuroscience: the Official Journal of the Society for Neuroscience. 2005; 25: 1904–1913. https://doi.org/10.1523/JNEUROSCI.4540-04.2005.

[19] Javed H, Azimullah S, Haque ME, Ojha SK. Cannabinoid Type 2 (CB2) Receptors Activation Protects against Oxidative Stress and Neuroinflammation Associated Dopaminergic Neurodegeneration in Rotenone Model of Parkinson's Disease. Frontiers in Neuroscience. 2016; 10: 321. https://doi.org/10.3389/fnins.2016.00321.

[20] Rousseaux C, Thuru X, Gelot A, Barnich N, Neut C, Dubuquoy L, *et al*. Lactobacillus acidophilus modulates intestinal pain and induces opioid and cannabinoid receptors. Nature Medicine. 2007; 13: 35–37. https://doi.org/10.1038/nm1521.

[21] Jiao Q, Liu J, Zhou L, McClements DJ, Liu W, Luo J, *et al*. *Lactobacillus* extracellular vesicles alleviate alcohol-induced liver injury in mice by regulating gut microbiota and activating the Nrf-2 signaling pathway. Food & Function. 2025; 16: 1284–1298. https://doi.org/10.1039/d4fo04364b.

[22] Chen Z, Zhong C. Oxidative stress in Alzheimer's disease. Neuroscience Bulletin. 2014; 30: 271–281. https://doi.org/10.1007/s12264-013-1423-y.

[23] Peña-Bautista C, Vigor C, Galano JM, Oger C, Durand T, Ferrer I, *et al*. Plasma lipid peroxidation biomarkers for early and non-invasive Alzheimer Disease detection. Free Radical Biology & Medicine. 2018; 124: 388–394. https://doi.org/10.1016/j.freeradbiomed.2018.06.038.

[24] Jakaria M, Belaidi AA, Bush AI, Ayton S. Ferroptosis as a mechanism of neurodegeneration in Alzheimer's disease. Journal of Neurochemistry. 2021; 159: 804–825. https://doi.org/10.1111/jnc.15519.

[25] Ashraf A, Jeandriens J, Parkes HG, So PW. Iron dyshomeostasis, lipid peroxidation and perturbed expression of cystine/glutamate antiporter in Alzheimer's disease: Evidence of ferroptosis. Redox Biology. 2020; 32: 101494. https://doi.org/10.1016/j.redox.2020.101494.

[26] Yu X, Li S, Yang D, Qiu L, Wu Y, Wang D, *et al*. A novel strain of Lactobacillus mucosae isolated from a Gaotian villager improves in vitro and in vivo antioxidant as well as biological properties in D-galactose-induced aging mice. Journal of Dairy Science. 2016; 99: 903–914. https://doi.org/10.3168/jds.2015-10265.

[27] Estrada JA, Contreras I. Endocannabinoid Receptors in the CNS: Potential Drug Targets for the Prevention and Treatment of Neurologic and Psychiatric Disorders. Current Neuropharmacology. 2020; 18: 769–787. https://doi.org/10.2174/1570159X

18666200217140255.
[28] Solas M, Francis PT, Franco R, Ramirez MJ. CB2 receptor and amyloid pathology in frontal cortex of Alzheimer's disease patients. Neurobiology of Aging. 2013; 34: 805–808. https://doi.org/10.1016/j.neurobiolaging.2012.06.005.
[29] Wu J, Hocevar M, Foss JF, Bie B, Naguib M. Activation of CB_2 receptor system restores cognitive capacity and hippocampal Sox2 expression in a transgenic mouse model of Alzheimer's disease. European Journal of Pharmacology. 2017; 811: 12–20. https://doi.org/10.1016/j.ejphar.2017.05.044.
[30] Wu J, Bie B, Yang H, Xu JJ, Brown DL, Naguib M. Activation of the CB2 receptor system reverses amyloid-induced memory deficiency. Neurobiology of Aging. 2013; 34: 791–804. https://doi.org/10.1016/j.neurobiolaging.2012.06.011.
[31] Tao H, Li X, Chu M, Wang Q, Li P, Han Q, *et al*. CB2 regulates oxidative stress and osteoclastogenesis through NOX1-dependent signaling pathway in titanium particle-induced osteolysis. Cell Death Discovery. 2023; 9: 461. https://doi.org/10.1038/s41420-023-01761-y.
[32] Cheng X, Lin J, Chen Z, Mao Y, Wu X, Xu C, *et al*. CB2-mediated attenuation of nucleus pulposus degeneration via the amelioration of inflammation and oxidative stress in vivo and in vitro. Molecular Medicine (Cambridge, Mass.). 2021; 27: 92. https://doi.org/10.1186/s10020-021-00351-x.
[33] Paloczi J, Varga ZV, Hasko G, Pacher P. Neuroprotection in Oxidative Stress-Related Neurodegenerative Diseases: Role of Endocannabinoid System Modulation. Antioxidants & Redox Signaling. 2018; 29: 75–108. https://doi.org/10.1089/ars.2017.7144.
[34] Aso E, Juvés S, Maldonado R, Ferrer I. CB2 cannabinoid receptor agonist ameliorates Alzheimer-like phenotype in AβPP/PS1 mice. Journal of Alzheimer's Disease: JAD. 2013; 35: 847–858. https://doi.org/10.3233/JAD-130137.
[35] Zhang M, Zhang M, Wang L, Yu T, Jiang S, Jiang P, *et al*. Activation of cannabinoid type 2 receptor protects skeletal muscle from ischemia-reperfusion injury partly via Nrf2 signaling. Life Sciences. 2019; 230: 55–67. https://doi.org/10.1016/j.lfs.2019.05.056.